

1 **Title:** The cellular and molecular landscape of hypothalamic patterning and
2 differentiation.

3
4 **Authors:** Dong Won Kim¹, Parris Whitney Washington^{1*}, Zoe Qianyi Wang^{1*}, Sonia
5 Hao Lin^{1*}, Changyu Sun¹, Basma Taleb Ismail¹, Hong Wang¹, Lizhi Jiang¹, and Seth
6 Blackshaw¹⁻⁶.

7
8 **Affiliations:** ¹Solomon H. Snyder Department of Neuroscience, ²Department of
9 Ophthalmology, ³Department of Neurology, ⁴Center for Human Systems Biology,
10 ⁵Institute for Cell Engineering, ⁶Kavli Neuroscience Discovery Institute, Johns Hopkins
11 University School of Medicine, Baltimore, MD, 21205, USA.

12 *These authors contributed equally.

13 Address all correspondence to sblack@jhmi.edu (S.B.)

14
15 **Abstract:**

16 The hypothalamus is a central regulator of many innate behaviors essential for survival,
17 but the molecular mechanisms controlling hypothalamic patterning and cell fate
18 specification are poorly understood. To identify genes that control hypothalamic
19 development, we have used single-cell RNA sequencing (scRNA-Seq) to profile mouse
20 hypothalamic gene expression across 12 developmental time points between embryonic
21 day 10 and postnatal day 45. This identified genes that delineated clear developmental
22 trajectories for all major hypothalamic cell types, and readily distinguished major
23 regional subdivisions of the developing hypothalamus. By using our developmental
24 dataset, we were able to rapidly annotate previously unidentified clusters from existing
25 scRNA-Seq datasets collected during development, and to identify the developmental
26 origins of major neuronal populations of the ventromedial hypothalamus. We further
27 show that our approach can rapidly and comprehensively characterize mutants that
28 have altered hypothalamic patterning, identifying *Nkx2.1* as a negative regulator of
29 prethalamic identity. These data serve as a resource for further studies of hypothalamic
30 development, physiology and dysfunction.

31
32 **Introduction:**

33 The hypothalamus is comprised of a diverse array of neuronal and glial cell
34 types, many of which are organized into spatially discrete clusters or nuclei¹⁻³.
35 Stereotactic lesion and focal stimulation studies have identified individual nuclei as
36 essential for regulating a broad range of homeostatic physiological processes, ranging
37 from circadian rhythms to hunger; behaviors such as mating, aggression and care of
38 young; and cognitive processes such as motivation, reward, and memory⁴⁻⁷. More
39 recently, opto- and chemogenetic techniques have made it possible to identify the role
40 of individual hypothalamic neuronal subtypes in controlling some of these behaviors⁸⁻¹⁰.
41 Progress in this area has been hampered, however, by the fact that hypothalamic
42 cell types thus far have remained quite poorly characterized, despite recent efforts
43 aimed at using scRNA-Seq to classify cells in certain hypothalamic regions¹¹⁻¹⁴. Still
44 less is known about how hypothalamic cell types acquire their identities during
45 development. Even the basic spatial organization of the developing hypothalamus, and
46 its relationship to other forebrain structures such as the prethalamus and telencephalon,

47 remains contentious^{15–17}. Previous efforts using microarray analysis coupled with large-
48 scale two-color *in situ* hybridization have identified a set of molecular markers that
49 uniquely define spatial domains of the early embryonic hypothalamus and adjacent
50 diencephalic regions², while parallel efforts using high-throughput *in situ* hybridization
51 have identified additional region-specific markers^{18,19}.

52 These datasets have been used as the basis for genetic studies that selectively
53 disrupt development of specific hypothalamic regions and/or cell types^{20–24}, leading to
54 identification of novel functions for previously characterized hypothalamic regions or cell
55 types^{25,26}. However, these datasets have important limitations: they do not provide
56 cellular resolution of gene expression data, and they do not efficiently measure
57 coexpression of multiple genes. In addition, despite the availability of many highly
58 specific molecular markers, analysis of mutants that affect hypothalamic development is
59 currently both slow and difficult, owing to the complexity of this structure.

60 Recent advances in single-cell RNA-Seq technology (scRNA-Seq)²⁷ have made
61 it possible to both analyze the development of complex organs at cellular resolution and
62 to also rapidly and comprehensively characterize the molecular phenotype of
63 developmental mutants²⁸. In this study, we use scRNA-Seq to profile changes in gene
64 expression and cell composition across the full course of mouse hypothalamic
65 development, with a particular focus on identifying genes that control glial differentiation
66 and function. We next focus on identifying genes that control hypothalamic
67 regionalization and neurogenesis in the early embryo, and integrate these findings to
68 generate a *Hypothalamic Developmental Database* (HyDD), which identifies selective
69 markers of each region of the developing hypothalamus and prethalamus. We next use
70 the HyDD to rapidly annotate cell types in previously published scRNA-Seq datasets,
71 and to infer the developmental history of specific subtypes of adult hypothalamic
72 neurons. Finally, we demonstrate how the HyDD can be used to comprehensively
73 analyze developmental mutants that generate complex phenotypes that would be
74 difficult to characterize with traditional histology-based approaches, and in the process
75 identify *Nkx2-1* as a negative regulator of prethalamic identity.

76 This study provides a reference atlas for future studies of hypothalamic
77 development. It also identifies pathways by which gene regulatory networks that control
78 cell identity can be targeted to analyze the functional role of individual hypothalamic
79 neuronal subtypes.

80

81

Results:

82

Comprehensive profiling of entire course of hypothalamus development

83

84

85

86

87

88

89

90

91

92

To profile changes in gene expression across the full course of mouse
hypothalamic development, we processed 12 time points ranging from embryonic day
(E)10 to postnatal day (P)45. For E10-E16, both prethalamus and hypothalamus were
collected, whereas for E18-P45, only hypothalamus was profiled (Fig. 1a). In total,
129,151 cells were profiled (Fig. S1a,b). Using molecular markers of known
hypothalamic regions and cell types², we were able to annotate all major hypothalamic
and adjacent brain regions, and major cell types at each individual age (Fig. S1c,d).
Aggregation of the entire dataset with UMAP shows a clear developmental progression
from neuroepithelial cells at E10, hypothalamic patterning between E11 and E13, and to
the detection of major cell types in the mature hypothalamus (Fig. S2a). Roughly

93 similar detection of expressed genes and total mRNAs were observed at each time
94 point (Fig. S2b,c).

95 Trajectories leading from neuronal progenitors to mature glutamatergic and
96 GABAergic neurons, glia, ependymal cells and tanycytes were observed, as were
97 separate clusters representing hematopoietic, microglial and endothelial cells (Fig. 1b).
98 A separate cluster of oligodendrocytes was observed from P4 onwards, marked by a
99 high and selective expression of *Glul* (Fig. 1c). Oligodendrocytes from posterior brain
100 regions have been recently reported to selectively express high levels of *Glul*²⁹,
101 suggesting that these cells may migrate into the early postnatal hypothalamus from a
102 more posterior location. Abundant expression of hypothalamic neuropeptides including
103 *Pomc*, *Agrp*, *Ghrh*, *Sst*, *Gal*, *Hcrtr*, and *Pmch* were observed in the neuronal cluster (Fig.
104 S3).

105 Glial cells of the hypothalamus have been shown to play critical and tissue-
106 specific roles in regulation of osmolarity³⁰, circadian rhythm³¹, metabolism³² and
107 neurogenesis³³. To better understand the molecular mechanisms controlling the
108 specification and differentiation of hypothalamic glia, each glial population was re-
109 clustered and examined separately.

110 Cells that were identified as part of the oligodendrocyte maturation trajectory, and
111 hence that share a similar molecular history, were re-clustered as previously
112 described^{13,34}, and genes that demarcate each stage of oligodendrocyte development
113 were identified (Fig. S4a-c, Table S1). To identify genes selectively enriched in
114 hypothalamic oligodendrocytes, mature oligodendrocytes were directly compared to
115 scRNA-Seq datasets from mature cortical oligodendrocytes. While *Pcsk1n* and *Cbx3*
116 are highly enriched in hypothalamic, relative to cortical, oligodendrocytes (Fig. S4d-h),
117 these genes are enriched in all hypothalamic glial cells, and are not specific to
118 oligodendrocytes.

119 In contrast, we identified many genes that were both astrocyte-enriched relative
120 to other glial cell types, and selectively expressed in hypothalamic, relative to cortical,
121 astrocytes (Fig. S5a-c). These include higher expression of *Agt*, and a lower level of
122 *Mfge8* in hypothalamic astrocytes, as previously reported³⁴, along with newly identified
123 hypothalamic-enriched genes such as *Marcks* and *Marcks1* (Fig. S5a-c), which are
124 important regulators of protein kinase C-dependent calmodulin signaling^{35,36}.

125 Analysis of the developmental trajectory connecting gliogenic progenitor cells
126 and hypothalamic astrocytes identified transitional states between these two
127 populations. Immature hypothalamic astrocytes co-express the mature astrocyte
128 marker *Agt*, and *Rgcc*, a cell-cycle regulator that regulates Notch signaling^{37,38} (Fig.
129 S5d-f, Table S2). Loss of expression of genes specific to gliogenic progenitors was
130 observed in hypothalamic astrocytes and other glial populations after the second
131 postnatal week (Fig. S5g). Up-regulation of Notch signaling pathway components was
132 also observed, as previously reported for human astrocyte development *in vitro*³⁹ (Fig.
133 S5h).

134 Analysis of developmental trajectories for individual hypothalamic cell types
135 identified the age at which these cell types began to diverge in gene expression, and
136 identified both known and candidate regulators of cell fate. This is clearly seen when
137 comparing the development of two ventricular glial-like cell populations -- ependymal
138 cells and tanycytes. These two classes of ventricular cells begin to diverge at E13, with

139 differential expression of *Foxj1* and *Rax*, markers of ependymal cells and tanycytes, first
140 detected at this age (Fig. 1d, Fig. S6). Pseudotime analysis using BEAM analysis
141 identifies additional transcription factors that are candidates for controlling tanycyte and
142 ependymal cell specification and differentiation (Fig. S6a,b, Table S3). Tanycytes are
143 themselves heterogenous, and can be subdivided into alpha and beta subtypes based
144 on both spatial location and molecular markers^{13,40}. To determine whether transcription
145 factors enriched in differentiating tanycytes might also control tanycyte subtype
146 specification, we analyzed previously published scRNA-Seq data obtained from mature
147 tanycytes¹⁴ (Fig. S6c, d), and identified multiple tanycyte subtype-specific transcription
148 factors that are expressed during early stages of tanycyte differentiation, and hence are
149 strong candidates for controlling tanycyte subtype specification.

150

151 **Identification of genes selectively expressed in different regions of the** 152 **developing hypothalamus and prethalamus scRNA-Seq**

153 We next investigated whether we could use this dataset to faithfully distinguish
154 hypothalamic domains that are spatially distinct in the embryo. To do this, we re-
155 clustered data from E11, E12, and E13, which correspond to the peak period of
156 hypothalamic neurogenesis (Fig. 2a)⁴¹. Using previously identified region-specific
157 markers as a reference², we observed a clear segregation of spatially-distinct neuronal
158 precursors and progenitors (Fig. 2b, S7). We were able to readily distinguish
159 hypothalamic and adjacent cell populations including the prethalamus, discrete clusters
160 for telencephalic structures such as preoptic area and medial ganglionic eminence,
161 thalamic eminence, rim domain, and main body of the sensory thalamus, as well as the
162 zona limitans intrathalamica (ZLI) at all three developmental ages (Fig. 2b, S7-S8).

163 Each of the previously reported major subdivisions of the developing
164 hypothalamus² were also identified, including postmitotic neuronal precursor cells of the
165 paraventricular nucleus/supraoptic nucleus (PVN/SON), extrahypothalamic diagonal
166 (ID) and tuberomammillary terminal (TT), ventromedial hypothalamus (VMH), arcuate
167 nucleus (ARC), premammillary hypothalamus (PMN), mammillary nucleus (MMN), and
168 supramammillary nucleus (SMN) (Fig. 2c,d, S7). In addition, several spatially distinct
169 subtypes of mitotic hypothalamic progenitor cells were also observed, most notably cells
170 that shared markers of both MMN and SMN (Fig. 2d, Table S4).

171 Multiple known and previously undescribed molecular markers, including many
172 transcription factors, were identified for each of these regions (Fig. 2c, Table S4).
173 While some of these markers are shared among multiple regions in the hypothalamus
174 and other forebrain regions, others are highly specific and non-overlapping. We
175 identified clear separation between mitotic neural progenitors and postmitotic neural
176 precursors (Fig. 2d, S7).

177 This analysis was able to efficiently identify gene expression patterns that were
178 restricted to specific spatial domains and subdomains of the developing hypothalamus
179 and prethalamus, confirming and extending our previous findings². However, this
180 approach does not allow us to identify genes with more complex expression patterns,
181 but which nevertheless may play important roles in regulating hypothalamic
182 neurogenesis. To address this, we used scCoGAPS, a non-negative matrix
183 factorization tool that allows unbiased identification of patterns of co-expressed genes⁴²
184 (Fig. S8). Using this method, we identified patterns that not only matched key spatial

185 subdivisions of the hypothalamus and prethalamus, but also patterns that labeled
186 discrete subsets of hypothalamic progenitors (Table S5). These include hypothalamic
187 neural precursor cells (NPC) that likely correspond to radial glia (*Fabp7*, *Slc1a3*), as
188 well as neurogenic progenitors (*Pitx2*, *Nhlh1*, *Nhlh2*). Most strikingly, we observed
189 multiple patterns that selectively label neurogenic progenitors that are located along the
190 borders of the hypothalamus and prethalamus with both the telencephalon and ZLI.
191 Genes that drive this pattern include *Neurog2*, *Lhx5*, and *Nhlh2* (Table S5). Although
192 these expression patterns have been previously reported², the fate of these border cells
193 is unknown.

194 Due to the high complexity of the hypothalamic clusters observed in both two-
195 and three-dimensional analysis, it is difficult to comprehensively visualize region-specific
196 differences in gene expression. To improve visualization of these data, we generated a
197 heatmap for major pattern marker genes that corresponds to the two-dimensional
198 sagittal plane, capturing the main spatial subdivisions of the developing hypothalamus
199 and adjacent brain regions (Fig. S9).

200 This analysis also identified clusters that correspond to three hypothalamic
201 regions that had not been described in previous work², including two populations of
202 excitatory neurons. The first of these regions is found in the dorsomedial
203 hypothalamus, and is marked by expression of *Sst*, *Cited1*, *Otp* and *Six6* (Fig. 2c). The
204 second region is found in the TT/PMN region, and expresses *Pax7* (Table. S4). The
205 third region is found in the lateral hypothalamus (LH), and consists of a diverse
206 collection of subtypes of neuronal precursors. This LH cluster consists primarily of
207 glutamatergic neurons, with a small subpopulation of GABAergic neurons (Fig. S10,
208 Table S6). The glutamatergic population includes a discrete subcluster of *Lhx9*-positive
209 neurons, which marks precursors of hypocretin neurons^{2,43,44}. Cells within this LH
210 cluster express multiple transcription factors that are also selectively expressed in other
211 hypothalamic regions, including the VMH, PMN, MMN and ID.

212 Clustering of previously characterized spatial domains also identified discrete
213 subclusters that express common sets of genes. This is clearly seen in the PVN/SON
214 cluster (Fig. S11, Table S6). Selective expression of *Onecut2*, *Cartpt* and *Zic1*
215 characterizes a ventrolateral domain that, based on its position, likely corresponds to
216 the developing SON (Fig. S11). This same approach can be readily applied to other
217 forebrain regions. We have previously identified molecular markers that both identify
218 discrete spatial domains within the prethalamus, which gives rise to structures such as
219 the thalamic reticular nucleus and ventral lateral geniculate nucleus^{2,45,46}, and
220 investigated whether these regions could be identified using scRNA-Seq data.

221 Sub-clustering of prethalamic cells allowed us to detect these and other spatial
222 subdivisions within the prethalamus. We observed partially overlapping domains of
223 expression of the transcription factors *Sp8* and *Sp9* (Fig. S12, Table S6), which play
224 critical roles in the development of telencephalic interneurons⁴⁷. *In situ* hybridization
225 analysis revealed enriched expression of *Sp8* and *Lhx1* in anterior prethalamus and ID,
226 while *Sp9* and *Prox1* were enriched in posterior prethalamus (Fig. S12). *Zic1* and *Ebf1*
227 also marked distinct, but partially overlapping spatial domains in prethalamus (Fig. S12).

228 Sub-clustering of the VMH allowed us to detect two distinct clusters, which
229 corresponded to separate anterior and posterior domains of gene expression (Fig. S13,
230 Table S6). A clear distinction between these anterior and posterior domains was

231 detected until E16, both spatially and at the molecular level (Fig. S13). These two
232 clusters had begun to spatially intermingle, yet the molecular distinction still remained,
233 possibly reflecting local tangential cell migration within the VMH.

234 By combining our analysis of both the molecular markers of differentiation of
235 major hypothalamic cell types and the selective markers of the different spatial domains
236 of the developing hypothalamus and prethalamus, we have compiled a reference set of
237 molecular markers that will be useful for further functional studies. We have
238 designated this integrated and annotated scRNA-Seq dataset as a HyDD, or the
239 *Hypothalamus Developmental Database*.

240

241 **HyDD can rapidly annotate existing hypothalamus scRNA-Seq dataset and** 242 **identifies developmental origins of VMH neurons**

243 To demonstrate the broad usefulness of the HyDD, we first annotated a
244 previously published scRNA-Seq dataset obtained through selective dissection of
245 *Pomc-EGFP*-expressing cells from E15.5 hypothalamus using regional and cell type-
246 specific markers from the HyDD⁴⁸. In this study, while one cluster (cluster 0) was
247 previously identified as the developing ARC, the remaining clusters were not annotated
248 owing to the lack of well defined regional and cell type-specific markers to resolve
249 spatial location of these clusters. Using markers obtained from the HyDD to train the
250 dataset, we were able to annotate all but two clusters, representing cells from multiple
251 hypothalamic regions, including VMH, PMH, anterior ID, DMH, SCN, and ARC. Some
252 clusters were composed of cells from multiple hypothalamic regions, which may explain
253 some of the previous difficulties in annotating these cells (Fig. 3a,b). Two unannotated
254 clusters appear to reflect contamination from the habenula and pituitary that occurred
255 during dissection (Fig. S14). A subset of the neurons in the ARC cluster share
256 molecular markers of neural precursors in the PMN and DMH, implying that these cells
257 may have migrated to the ARC from these regions (Fig. S14).

258 We also identified a cluster that closely resembled hypothalamic NPC (Fig. S15),
259 but which also co-expressed astrocyte-, ependymal and/or tanyocyte-specific marker
260 genes. Gene sets enriched in this cluster were then projected into the entire
261 hypothalamus scRNA-Seq dataset (E10-P45), and glial populations including immature
262 glial cells were enriched with these gene sets. This same gene expression pattern was
263 found to be enriched in a subset of hypothalamic NPC that were detected from E11
264 onwards, and which may represent NPC that are competent to generate glia (Fig. S15).
265 Many of these same genes are also expressed in the late-stage retinal progenitor cells,
266 from the age at which they become competent to give rise to tanyocyte-like Müller glial
267 cells²⁸.

268 Since HyDD contains a nearly uninterrupted temporal profile of changes in gene
269 expression during the process of cell specification and differentiation, HyDD can also be
270 used to infer the developmental origins of fully mature hypothalamic neurons. However,
271 identifying the precise spatial location of individual cell types from hypothalamus
272 scRNA-Seq data based on specific molecular markers alone is bioinformatically
273 challenging, due to the extreme tissue complexity. This is the case even when scRNA-
274 Seq data has been generated with micro-dissected or flow-sorted cells from pre-defined
275 hypothalamic regions. Most informative region-specific markers are strongly expressed
276 early in development, but are either not expressed or show substantially different

277 expression levels at later developmental ages⁴⁹. Postmitotic hypothalamic neural
278 precursors also undergo a considerable amount of tangential migration and dispersion,
279 making it even harder to directly identify gene regulatory networks that control the
280 specification of individual hypothalamic cell types⁵⁰.

281 To identify the developmental origin of individual hypothalamic cell types, it is
282 critical that overlapping sets of markers be identified that selectively label each stage of
283 cell differentiation, in a manner analogous to molecular stepping stones, so that the
284 developmental history of each cell type can be reconstructed. As a proof of principle for
285 this approach, we identified gene sets that identify VMH cells at early stages of
286 hypothalamic development (Fig. 3C), when region-specific molecular markers are
287 robustly expressed. Gene sets specific to discrete spatial domains were then used to
288 train the following developmental age to find VMH cells and new VMH-enriched genes
289 were identified. This process was repeated for each successive developmental age.
290 These VMH-enriched genes have varying levels of expression and specificity across the
291 full course of the hypothalamus development (Fig. S16).

292 We next used the HyDD to identify the developmental origin of major VMH
293 neuronal subtypes. Recent scRNA-Seq of the adult VMH identified multiple clusters of
294 both core glutamatergic VMH neurons and of GABAergic neurons surrounding the core
295 VMH (VMH-out)⁵¹. We sought to identify the developmental origins of both classes of
296 VMH neurons. We first found that GABAergic neurons of VMH-out originated from four
297 distinct regions of the developing hypothalamus - ARC, DMH, Ant ID and PMN (Fig. 3d)
298 -- with each VMH-out GABAergic cluster having a distinct developmental origin based
299 on specific expression of regional markers. We likewise observed that different subsets
300 of core glutamatergic VMH neurons arise from distinct anterior or posterior domains of
301 the embryonic VMH (Fig. S13). Some of these clusters remain restricted to anterior or
302 posterior regions of the adult VMH, as noted in the original study⁵¹(Fig. 3d, Fig. S17a,b).
303 However, the majority of VMH neuronal subtypes originate from both anterior and
304 posterior domains of the developing VMH (Fig. S17), and are distributed widely along
305 the anterior-posterior axis of the adult VMH⁵¹. VMH neuronal subtypes may thus be two
306 distinct developmental steps: an initial stage in which anterior and posterior identity is
307 specified between E11 and E13, and a later stage that coincides with the initiation of
308 local tangential migration that occurs from E16 onwards.

309

310 **HyDD allow rapid and comprehensive analysis of complex mutant phenotypes** 311 **that alter hypothalamic and prethalamic patterning**

312 HyDD provides both a high-resolution molecular atlas of the developing
313 hypothalamus and prethalamus, and a useful resource to understand the developmental
314 origin of adult hypothalamic neurons. We next sought to determine if HyDD could also
315 be used to rapidly and comprehensively characterize mutants that regulate early stages
316 of hypothalamic development and organization. As proof of concept, we performed
317 scRNA-Seq analysis on E12.5 *Foxd1*^{CreGFP/+}; *Ctnnb1*^{ex3/+} mice, in which a constitutively
318 active form of beta-catenin is overexpressed in *Foxd1*-positive hypothalamic and
319 prethalamic progenitors, leading to activation of canonical Wnt signaling in these cells
320 and their descendants²⁰. The same analysis was also with *Foxd1*^{CreGFP/+} littermate
321 controls. These mice show broad activation of the canonical Wnt pathway effector
322 *Lef1*, a hyperplastic ventricular zone, and with the exception of a handful of posterior

323 hypothalamic markers, show the loss of most regional markers in the hypothalamus and
324 prethalamus²⁰.

325 ScRNA-Seq analysis of control and mutant animals at E12.5 reveals several
326 mutant-specific cell clusters (Fig. S18a). Using the HyDD to annotate both control and
327 mutant data, we identified changes in gene expression and cell composition that match
328 previously reported findings (Fig. 4a), where we observed a substantial increase in
329 undifferentiated NPC, along with a corresponding reduction in the number of cells
330 expressing markers of hypothalamic and prethalamic neuronal precursors (Fig. 4b,
331 S18). In particular, strong loss of markers shared by both hypothalamus and
332 prethalamus, such as *Arx*, *Isl1* and *Gad1/2* (Fig. S19, Table S7) was observed. We
333 also identified two cell clusters that are found exclusively in mutant mice, both of which
334 express NPC markers, and also highly express both *Lef1* and negative regulators of
335 canonical Wnt signaling such as *Dkk1*, *Wif1* and *Axin2* (Fig. S18e). One of these
336 clusters is strongly enriched for G2/M phase markers such *Ube2c*, *Rrm2*, and *Ccnb1*
337 (Fig. 4b). Flow cytometry data also demonstrated a substantially higher fraction of
338 NPCs in G2/M phase in mutant mice (Fig. S18f), as has been previously reported in
339 non-neuronal cells that show high levels of canonical Wnt signaling⁵². This finding
340 explains the previous observation that, although a massive increase in the number of
341 NPC cells is seen in these mutants, only a modest increase is observed in EdU labeling,
342 which labels S-phase NPC²⁰. This demonstrates the power of using scRNA-Seq in
343 conjunction with the HyDD to analyze developmental phenotypes, in a manner that is
344 far more rapid and comprehensive than conventional histological techniques.

345 We next used this same approach to characterize E12.5 *Nkx2-1^{CreER/CreER}* knock-
346 in mice, which are homozygous for a null allele in the homeodomain transcription factor
347 *Nkx2-1*⁵³. *Nkx2-1* is broadly and selectively expressed in ventral hypothalamic
348 progenitors, as well as in progenitors that give rise to telencephalic interneurons^{54,55}.
349 Loss of function of *Nkx2-1* leads to a substantial reduction in ventral hypothalamic
350 structures by E18⁵⁶, but a detailed molecular characterization of these mutants has not
351 been conducted.

352 Analysis of *Nkx2-1^{CreER/CreER}* mutants and heterozygous littermate controls
353 revealed changes in cluster densities in the mutant (Fig. S20). We observed a broad
354 loss of markers specific to *Nkx2-1* positive ventral hypothalamic structures such as
355 ARC, VMH, PMN, and MMN, but not the SMN (Fig. 4c,d, Fig. S21, Table S8, S9), with
356 both the relative expression levels and the number of cells expressing these markers
357 reduced. Both the width of the hypothalamic ventricular zone and the levels of EdU
358 incorporation were reduced in *Nkx2-1^{CreER/CreER}* mice (Fig. S22). An increase in the
359 fraction of cells expressing prethalamic markers was detected (Fig. 4d, Fig. S23), and
360 increased Cre expression was also observed in these mice.

361 In contrast to controls, prethalamic cells in mutant mice expressed *Cre*, implying
362 that ventral hypothalamic cells that normally express *Nkx2.1* may have acquired
363 prethalamic identity (Fig. S22). To investigate this further, RNAscope probes against
364 *Sp9*, *Meis2* and *Cre* were used to visualize the location of these *Cre*-positive
365 prethalamic cells, and substantial co-localization of prethalamic markers and *Cre*
366 expression was observed in the region normally occupied the by the ventral
367 hypothalamus in controls (Fig. S22). This implies that *Nkx2-1* not only maintains the
368 identity of ventral hypothalamic progenitors but also actively represses expression of

369 molecular markers of prethalamus identity. *In situ* hybridization confirmed that there was
370 an increase in the absolute size of the prethalamus and its proportion in the
371 diencephalon (Fig. S23). An increase in the number of cells expressing markers of
372 NPC in the SMN and MMN was also seen, while *Nkx2-1* negative hypothalamic regions
373 such as the PVN/SON are unaffected (Fig. 4d, S24).

374

375

Discussion:

376

377 In this study, we use scRNA-Seq to develop a molecular atlas of the developing
378 mouse hypothalamus, with a particular focus on stages when hypothalamic patterning
379 and neurogenesis are regulated. This dataset identifies genes that are selectively
380 expressed during the differentiation of major neuronal and non-neuronal hypothalamic
381 cell types, and accurately delineates spatial subdivisions present in the early stages of
382 development of both the hypothalamus and the adjacent prethalamus. It also identifies
383 many previously uncharacterized transcription factors and other genes that are
384 excellent candidates for controlling regional patterning and specification of individual
385 hypothalamic cell types. Combining functional analysis of these genes with the new
386 selective markers of hypothalamic regions and immature hypothalamic cell types
387 identified in this study has the promise to greatly expand our knowledge of hypothalamic
388 development and organization.

388

389

390

391

392

393

394

395

396

397

398

399

400

401

402

403

404

405

406

407

408

409

410

411

412

413

414

The integrated dataset presented here provides three specific features that are critical for studying the formation and function of the hypothalamus. First, it makes it straightforward to unambiguously annotate major cell types at all stages of hypothalamic development. Second, it makes it possible in many cases to infer the developmental histories of hypothalamic cells in both the developing and mature hypothalamus. Third, it allows rapid and accurate phenotyping of mutants that show broad effects on hypothalamic patterning, neurogenesis and differentiation, with which we were able to validate our findings using traditional histological analysis. Despite the availability of highly specific molecular markers for the major spatial subdivisions of the hypothalamus, the highly complex and temporally dynamic anatomy of this brain region makes analysis of mutant phenotypes slow and complex. Previously, it has taken up to several years of full-time labor to obtain detailed characterization of individual mutant lines. The HyDD dataset allows these analyses to be conducted far more rapidly, efficiently, and comprehensively.

Our scRNA-Seq characterization of *Nkx2-1*-deficient mice identifies an unexpected developmental connection between the hypothalamus and prethalamus, where *Nkx2-1* can potentially act as both a positive regulator of ventral hypothalamic identity while simultaneously repressing prethalamus identity. This result is not predicted by the current prosomeric model for forebrain organization^{57,58}, and raises questions about the early development and patterning of these structures. Previous models of hypothalamic development and organization were constructed using very sparse datasets - typically single color *in situ* hybridization of a limited number of genes at a small number of time points. The much richer datasets provided by scRNA-Seq, and interpreted using the HyDD data, offer a far more powerful resource for constructing these models..

415 **References:**

- 416 1. Bedont, J. L., Newman, E. A. & Blackshaw, S. Patterning, specification, and
417 differentiation in the developing hypothalamus. *Wiley Interdiscip. Rev. Dev. Biol.* **4**,
418 445–468 (2015).
- 419 2. Shimogori, T. *et al.* A genomic atlas of mouse hypothalamic development. *Nat.*
420 *Neurosci.* **13**, 767–775 (2010).
- 421 3. Xie, Y. & Dorsky, R. I. Development of the hypothalamus: conservation,
422 modification and innovation. *Development* **144**, 1588–1599 (2017).
- 423 4. Kent, M. A. & Peters, R. H. Effects of ventromedial hypothalamic lesions on hunger-
424 motivated behavior in rats. *J. Comp. Physiol. Psychol.* **83**, 92–97 (1973).
- 425 5. Kruk, M. R. *et al.* Discriminant analysis of the localization of aggression-inducing
426 electrode placements in the hypothalamus of male rats. *Brain Research* vol. 260
427 61–79 (1983).
- 428 6. Lammers, J. H., Kruk, M. R., Meelis, W. & van der Poel, A. M. Hypothalamic
429 substrates for brain stimulation-induced attack, teeth-chattering and social grooming
430 in the rat. *Brain Res.* **449**, 311–327 (1988).
- 431 7. Hervey, G. R. The effects of lesions in the hypothalamus in parabiotic rats. *J.*
432 *Physiol.* **145**, 336–352 (1959).
- 433 8. Bedont, J. L. *et al.* An LHX1-Regulated Transcriptional Network Controls
434 Sleep/Wake Coupling and Thermal Resistance of the Central Circadian
435 Clockworks. *Curr. Biol.* **27**, 128–136 (2017).
- 436 9. Kohl, J. *et al.* Functional circuit architecture underlying parental behaviour. *Nature*
437 **556**, 326–331 (2018).
- 438 10. Yang, T. *et al.* Social Control of Hypothalamus-Mediated Male Aggression. *Neuron*
439 **95**, 955–970.e4 (2017).
- 440 11. Romanov, R. A. *et al.* Molecular interrogation of hypothalamic organization reveals
441 distinct dopamine neuronal subtypes. *Nat. Neurosci.* **20**, 176–188 (2017).
- 442 12. Mickelsen, L. E. *et al.* Single-cell transcriptomic analysis of the lateral hypothalamic
443 area reveals molecularly distinct populations of inhibitory and excitatory neurons.
444 *Nat. Neurosci.* **22**, 642–656 (2019).
- 445 13. Chen, R., Wu, X., Jiang, L. & Zhang, Y. Single-Cell RNA-Seq Reveals
446 Hypothalamic Cell Diversity. *Cell Reports* vol. 18 3227–3241 (2017).
- 447 14. Campbell, J. N. *et al.* A molecular census of arcuate hypothalamus and median
448 eminence cell types. *Nat. Neurosci.* **20**, 484–496 (2017).
- 449 15. Swanson, L. W. *Brain Maps: Structure of the Rat Brain.* (Elsevier Publishing
450 Company, 1992).
- 451 16. Kuhlenbeck, H. *The Central Nervous System of Vertebrates: pt. 1. Structural*
452 *elements: biology of nervous tissue. pt. 2. Overall morphologic pattern.* (1967).
- 453 17. Rubenstein, J. L., Martinez, S., Shimamura, K. & Puelles, L. The embryonic
454 vertebrate forebrain: the prosomeric model. *Science* **266**, 578–580 (1994).

- 455 18. Visel, A., Thaller, C. & Eichele, G. GenePaint.org: an atlas of gene expression
456 patterns in the mouse embryo. *Nucleic Acids Res.* **32**, D552 (2004).
- 457 19. Lein, E. S. *et al.* Genome-wide atlas of gene expression in the adult mouse brain.
458 *Nature* **445**, 168–176 (2007).
- 459 20. Newman, E. A., Wu, D., Taketo, M. M., Zhang, J. & Blackshaw, S. Canonical Wnt
460 signaling regulates patterning, differentiation and nucleogenesis in mouse
461 hypothalamus and prethalamus. *Dev. Biol.* **442**, 236–248 (2018).
- 462 21. Newman, E. A. *et al.* Foxd1 is required for terminal differentiation of anterior
463 hypothalamic neuronal subtypes. *Dev. Biol.* **439**, 102–111 (2018).
- 464 22. Kurrasch, D. M. *et al.* The neonatal ventromedial hypothalamus transcriptome
465 reveals novel markers with spatially distinct patterning. *J. Neurosci.* **27**, 13624–
466 13634 (2007).
- 467 23. Lee, B. *et al.* Dlx1/2 and Otp coordinate the production of hypothalamic GHRH- and
468 AgRP-neurons. *Nat. Commun.* **9**, 2026 (2018).
- 469 24. Sokolowski, K. *et al.* Specification of select hypothalamic circuits and innate
470 behaviors by the embryonic patterning gene dbx1. *Neuron* **86**, 403–416 (2015).
- 471 25. Liu, K. *et al.* Lhx6-positive GABA-releasing neurons of the zona incerta promote
472 sleep. *Nature* **548**, 582–587 (2017).
- 473 26. Bedont, J. L. *et al.* Lhx1 controls terminal differentiation and circadian function of
474 the suprachiasmatic nucleus. *Cell Rep.* **7**, 609–622 (2014).
- 475 27. Stuart, T. & Satija, R. Integrative single-cell analysis. *Nature Reviews Genetics* vol.
476 20 257–272 (2019).
- 477 28. Clark, B. S. *et al.* Single-Cell RNA-Seq Analysis of Retinal Development Identifies
478 NFI Factors as Regulating Mitotic Exit and Late-Born Cell Specification. *Neuron*
479 (2019) doi:10.1016/j.neuron.2019.04.010.
- 480 29. Xin, W. *et al.* Oligodendrocytes Support Neuronal Glutamatergic Transmission via
481 Expression of Glutamine Synthetase. *Cell Rep.* **27**, 2262–2271.e5 (2019).
- 482 30. Choe, K. Y., Olson, J. E. & Bourque, C. W. Taurine release by astrocytes
483 modulates osmosensitive glycine receptor tone and excitability in the adult
484 supraoptic nucleus. *J. Neurosci.* **32**, 12518–12527 (2012).
- 485 31. Tso, C. F. *et al.* Astrocytes Regulate Daily Rhythms in the Suprachiasmatic Nucleus
486 and Behavior. *Curr. Biol.* **27**, 1055–1061 (2017).
- 487 32. Chowen, J. A. *et al.* The role of astrocytes in the hypothalamic response and
488 adaptation to metabolic signals. *Prog. Neurobiol.* **144**, 68–87 (2016).
- 489 33. Lee, D. A. *et al.* Tanycytes of the hypothalamic median eminence form a diet-
490 responsive neurogenic niche. *Nature Neuroscience* vol. 15 700–702 (2012).
- 491 34. Zeisel, A. *et al.* Molecular Architecture of the Mouse Nervous System. *Cell* **174**,
492 999–1014.e22 (2018).
- 493 35. Gallant, C., You, J. Y., Sasaki, Y., Grabarek, Z. & Morgan, K. G. MARCKS is a
494 major PKC-dependent regulator of calmodulin targeting in smooth muscle. *J. Cell*

- 495 *Sci.* **118**, 3595–3605 (2005).
- 496 36. El Amri, M., Fitzgerald, U. & Schlosser, G. MARCKS and MARCKS-like proteins in
497 development and regeneration. *J. Biomed. Sci.* **25**, 43 (2018).
- 498 37. Counts, S. E. & Mufson, E. J. Regulator of Cell Cycle (RGCC) Expression During
499 the Progression of Alzheimer’s Disease. *Cell Transplant.* **26**, 693–702 (2017).
- 500 38. Carrieri, F. A. *et al.* CDK1 and CDK2 regulate NICD1 turnover and the periodicity of
501 the segmentation clock. *EMBO Rep.* **20**, e46436 (2019).
- 502 39. Malik, N. *et al.* Comparison of the gene expression profiles of human fetal cortical
503 astrocytes with pluripotent stem cell derived neural stem cells identifies human
504 astrocyte markers and signaling pathways and transcription factors active in human
505 astrocytes. *PLoS One* **9**, e96139 (2014).
- 506 40. Goodman, T. & Hajihosseini, M. K. Hypothalamic tanycytes—masters and servants
507 of metabolic, neuroendocrine, and neurogenic functions. *Frontiers in Neuroscience*
508 vol. 9 (2015).
- 509 41. Shimada, M. & Nakamura, T. Time of neuron origin in mouse hypothalamic nuclei.
510 *Exp. Neurol.* **41**, 163–173 (1973).
- 511 42. Stein-O’Brien, G. L. *et al.* Decomposing cell identity for transfer learning across
512 cellular measurements, platforms, tissues, and species. *bioRxiv* 395004 (2018)
513 doi:10.1101/395004.
- 514 43. Liu, J. *et al.* Evolutionarily conserved regulation of hypocretin neuron specification
515 by Lhx9. *Development* **142**, 1113–1124 (2015).
- 516 44. Dalal, J. *et al.* Translational profiling of hypocretin neurons identifies candidate
517 molecules for sleep regulation. *Genes Dev.* **27**, 565–578 (2013).
- 518 45. Vue, T. Y. *et al.* Characterization of progenitor domains in the developing mouse
519 thalamus. *J. Comp. Neurol.* **505**, 73–91 (2007).
- 520 46. Jeong, Y. *et al.* Spatial and temporal requirements for sonic hedgehog in the
521 regulation of thalamic interneuron identity. *Development* **138**, 531–541 (2011).
- 522 47. Li, J. *et al.* Transcription Factors Sp8 and Sp9 Coordinately Regulate Olfactory Bulb
523 Interneuron Development. *Cereb. Cortex* **28**, 3278–3294 (2018).
- 524 48. Huisman, C. *et al.* Single cell transcriptome analysis of developing arcuate nucleus
525 neurons uncovers their key developmental regulators. *Nat. Commun.* **10**, 3696
526 (2019).
- 527 49. Shimogori, T. *et al.* A genomic atlas of mouse hypothalamic development. *Nat.*
528 *Neurosci.* **13**, 767–775 (2010).
- 529 50. Arnold-Aldea, S. A. & Cepko, C. L. Dispersion Patterns of Clonally Related Cells
530 during Development of the Hypothalamus. *Developmental Biology* vol. 173 148–161
531 (1996).
- 532 51. Kim, D.-W. *et al.* Multimodal Analysis of Cell Types in a Hypothalamic Node
533 Controlling Social Behavior. *Cell* vol. 179 713–728.e17 (2019).
- 534 52. Olmeda, D., Castel, S., Vilaró, S. & Cano, A. β -Catenin Regulation during the Cell

- 535 Cycle: Implications in G2/M and Apoptosis. *Molecular Biology of the Cell* vol. 14
536 2844–2860 (2003).
- 537 53. Taniguchi, H. *et al.* A resource of Cre driver lines for genetic targeting of GABAergic
538 neurons in cerebral cortex. *Neuron* **71**, 995–1013 (2011).
- 539 54. Du, T., Xu, Q., Ocbina, P. J. & Anderson, S. A. NKX2.1 specifies cortical
540 interneuron fate by activating Lhx6. *Development* **135**, 1559–1567 (2008).
- 541 55. Elias, L. A. B., Potter, G. B. & Kriegstein, A. R. A time and a place for nkx2-1 in
542 interneuron specification and migration. *Neuron* vol. 59 679–682 (2008).
- 543 56. Kimura, S. *et al.* The T/ebp null mouse: thyroid-specific enhancer-binding protein is
544 essential for the organogenesis of the thyroid, lung, ventral forebrain, and pituitary.
545 *Genes Dev.* **10**, 60–69 (1996).
- 546 57. Puellas, L. Forebrain Development: Prosomere Model. *Encyclopedia of*
547 *Neuroscience* 315–319 (2009) doi:10.1016/b978-008045046-9.01076-7.
- 548 58. Ferran, J. L., Puellas, L. & Rubenstein, J. L. R. Molecular codes defining
549 rostrocaudal domains in the embryonic mouse hypothalamus. *Frontiers in*
550 *Neuroanatomy* vol. 9 (2015).
- 551

552 **Contribution:** DWK, SB designed experiments. DWK, PWW, ZQW, BTI, SL, LJ, HW
553 performed experiments. DWK, PWW, ZQW, SL, CS analyzed data. All authors
554 contributed to writing the paper

555

556 **Acknowledgements:**

557 This work was supported by a grant from the NIH (DK108230) to S.B. We thank
558 Transcriptomics and Deep Sequencing Core at Johns Hopkins for sequencing all
559 scRNA-Seq libraries, Ross Flow Cytometry Core (Johns Hopkins) for FACS analysis,
560 and Microscope facility (Johns Hopkins MICFAC, supported by the award number
561 S10OD018118). We thank M. Placzek, E. Newman, J. Nathans, A. Kolodkin, W. Yap,
562 and members of the Blackshaw lab for comments on the manuscript.

563

564 **Data availability:**

565 All scRNA-Seq data are available on GEO, GSE132355. Data can be viewed at
566 <https://proteinpaint.stjude.org/F/mm10/example.scrna.html>.

567

568

569

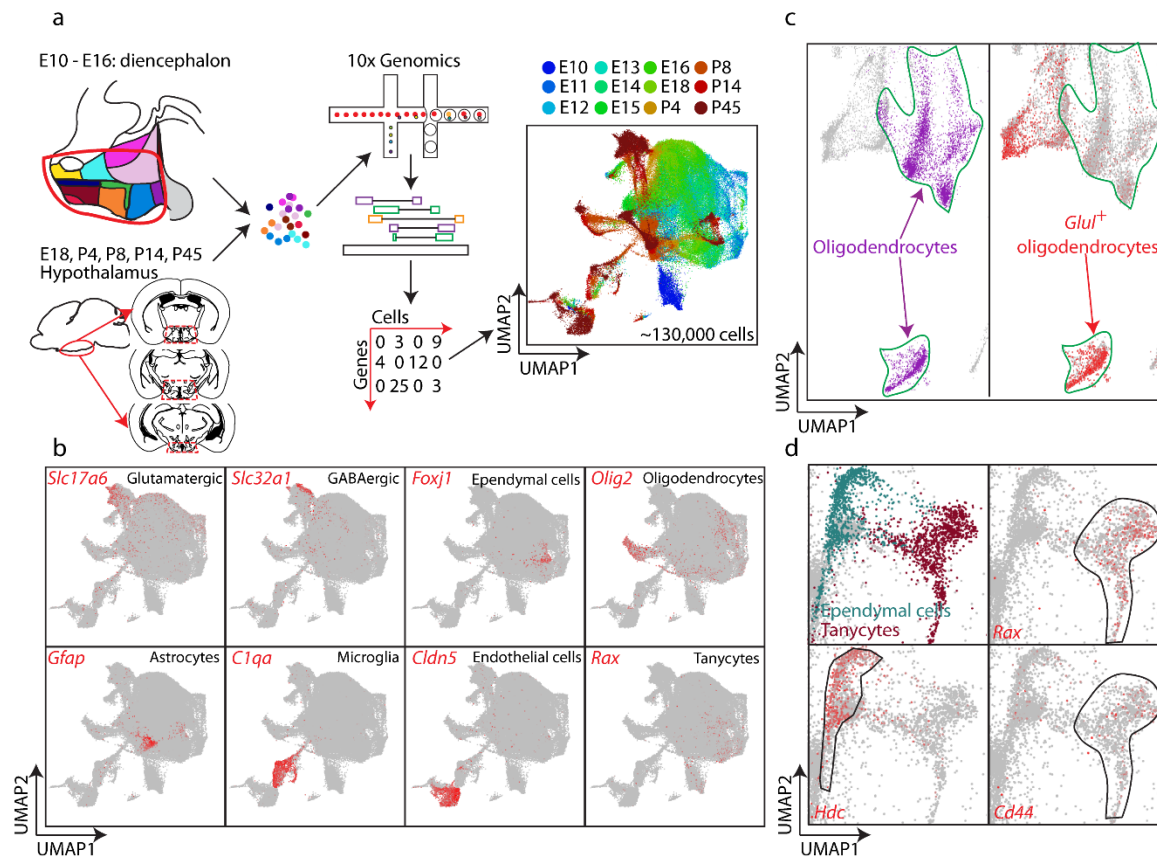


Fig1. Kim, et al.

Figure 1. Overview of generation of the hypothalamus scRNA-Seq dataset. (a) Schematic diagram showing overall experimental strategy. 12 time points of developing diencephalon including the prethalamus and hypothalamus (between E10 and E16), and hypothalamus (between E18 and P45) were profiled using the 10x Genomics Chromium system. Distribution of individual ages (blue = younger time point, red = older time point) is shown in the UMAP plot. (b) UMAP plot showing distribution of major cell types (red) of the hypothalamus at the terminal neuronal branch. (c) UMAP plot (higher power view) showing two separate populations of oligodendrocytes, *Glul*-positive and *Glul*-negative oligodendrocytes in the hypothalamus. (d) UMAP plot (higher power view) showing diverging developmental trajectories giving rise to leading to ependymal cells (green, *Hdc*) and tanycytes (brown, *Rax*, *Cd44*).

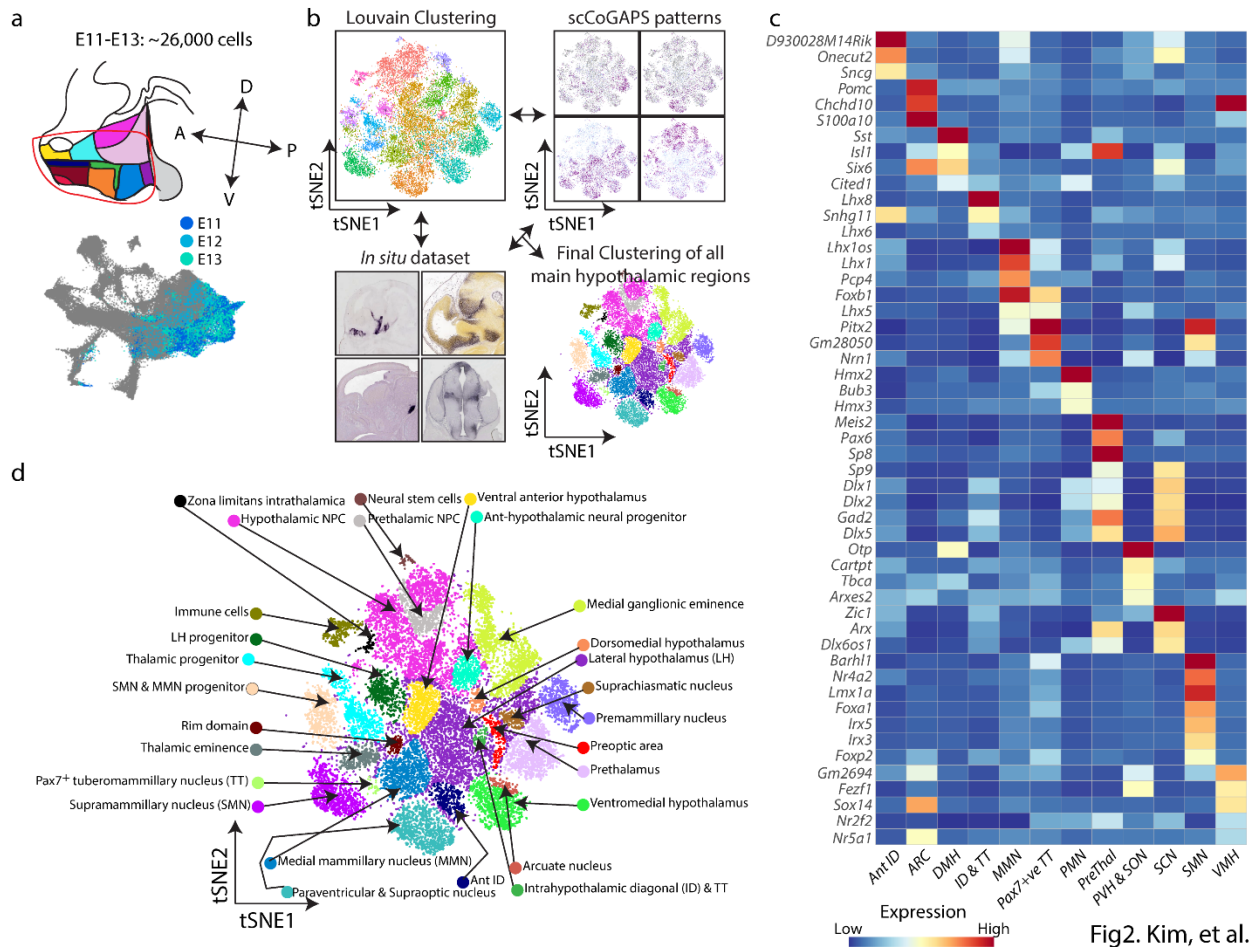


Fig2. Kim, et al.

Figure 2. Specification of hypothalamic patterning during embryonic development.

(a) Schematic diagram showing extraction of E11, E12 and E13 data to perform detailed analysis on hypothalamic patterning during development. (b) tSNE plot showing major subdivisions of the developing diencephalon (prethalamus and hypothalamus) and nearby regions to the developing diencephalon that are derived by cross-validation using the Louvain clustering algorithm, patterns from scCoGAPS and *in situ* analysis. (c) Heatmap showing a key subset of pattern-specific genes in major hypothalamic regions and prethalamus. (d) tSNE plot of E11-E13 developing diencephalon and adjacent regions.

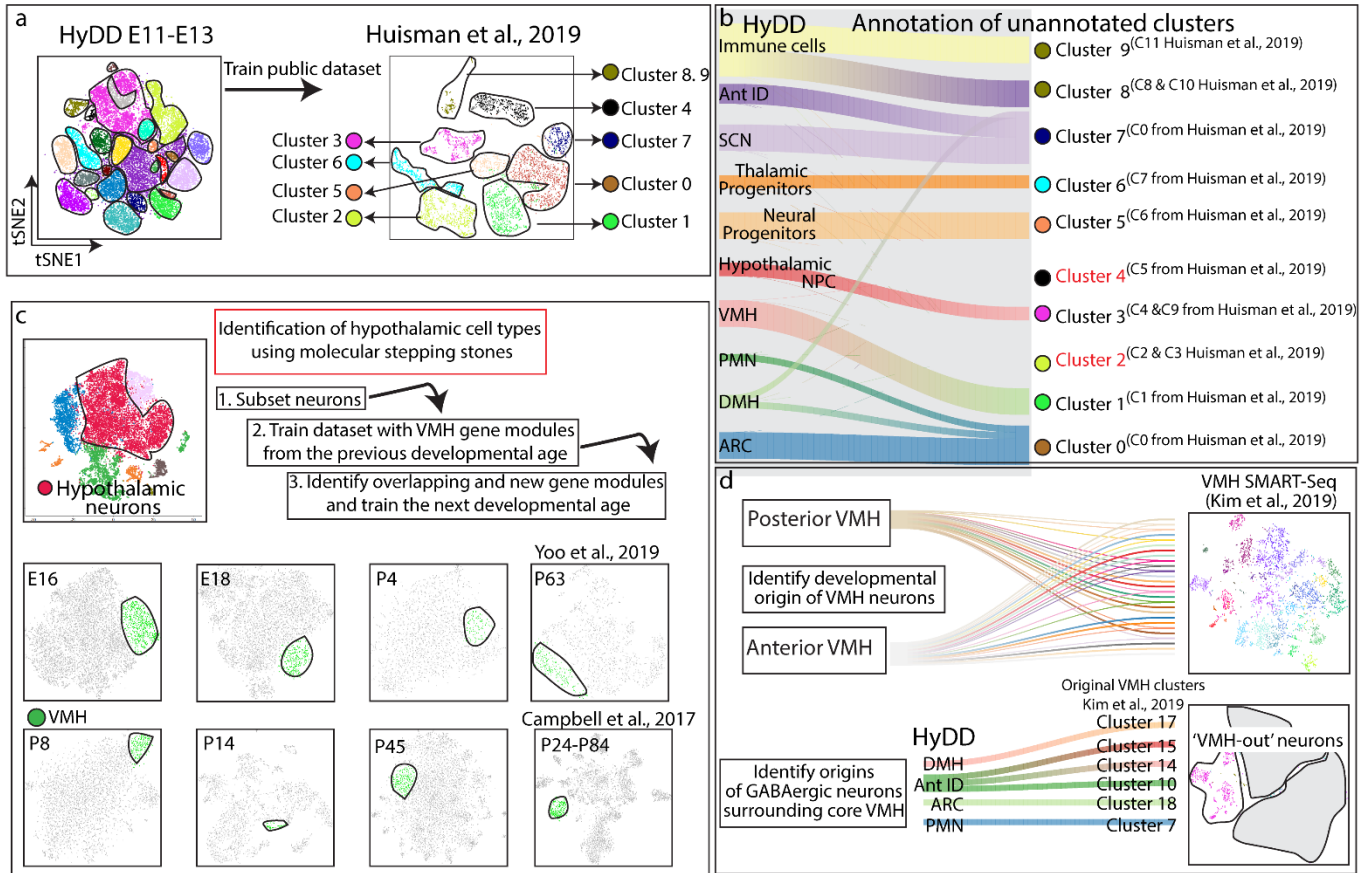


Fig3. Kim, et al.

Figure 3. Utilizing HyDD to infer the identity and origin of individual cell types in the developing and adult hypothalamus. (a) The HyDD dataset was used to train a previously published scRNA-Seq on E15.5 hypothalamus obtained through selective dissection of *Pomc-EGFP*-expressing cells⁴⁸. (b) Alluvial plot showing HyDD clusters (left) matched to clusters from Huisman et al., 2019⁴⁸ (right). Note that 2 clusters (clusters 2 and 4) from Huisman et al., 2019⁴⁸ do not match the HyDD dataset. (c) Using the molecular stepping stone approach to identify VMH neurons (green) across the entire developmental ages by identification of shared sets of gene modules that can demarcate the VMH across the entire hypothalamus scRNA-Seq dataset. (d) HyDD dataset is used to identify the developmental origins of previously annotated subtypes of glutamatergic neurons of the core VMH⁵¹ (top), and to identify the developmental origins of GABAergic neurons surrounding the core VMH (bottom).

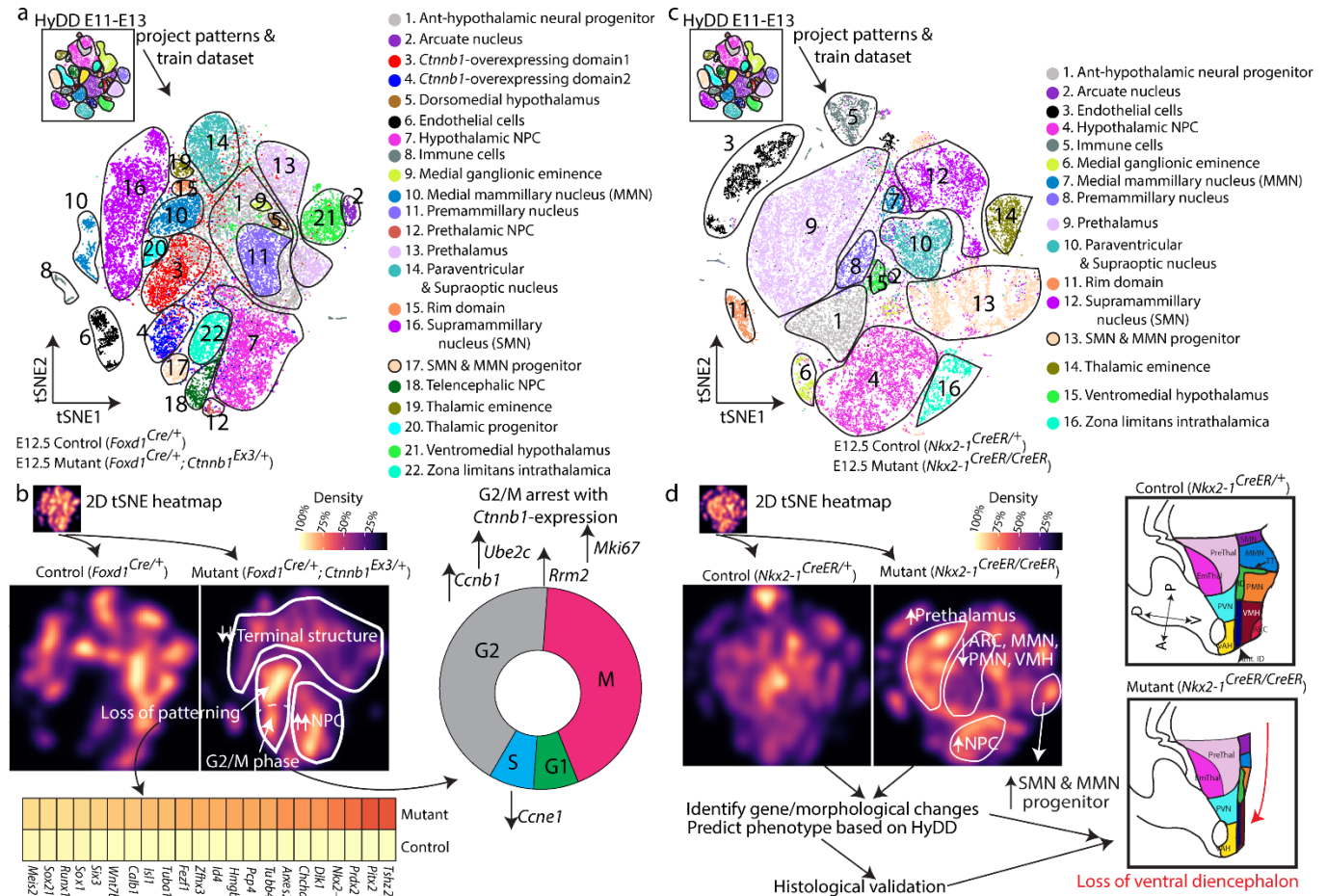


Fig4. Kim, et al.

Figure 4. scRNA-Seq can be used to screen mutant phenotype in the hypothalamus. (a) tSNE showing distribution of diencephalic and nearby brain structures in control (*Foxd1*^{Cre/+}) and mice selectively overexpressing a constitutively active mutant form of *Ctnnb1* in neuroepithelial cells of the hypothalamus and prethalamus (*Foxd1*^{Cre/+}; *Ctnnb1*^{Ex3/+}) with clusters obtained by training the dataset with HyDD markers. Note distinct clusters (clusters 3 and 4) that are only observed in mutant samples²⁰. (b) tSNE heatmap showing distribution of individual cluster between control (*Foxd1*^{Cre/+}) and constitutively active *Ctnnb1* mutants (*Foxd1*^{Cre/+}; *Ctnnb1*^{Ex3/+}) (top left) and heatmap showing that mutant-specific clusters display all pattern-specific markers that are expressed across the developing diencephalon (bottom left), with a high level of G2/M phase markers in the mutant-specific cluster (right). (c) tSNE showing the distribution of hypothalamic, prethalamus and adjacent brain structures of control (*Nkx2-1*^{CreER/+}) and *Nkx2-1* mutant line (*Nkx2-1*^{CreER/CreER}) with clusters obtained by training the dataset with HyDD markers. (d) tSNE heatmap showing distribution of individual clusters between control (*Nkx2-1*^{CreER/+}) and *Nkx2-1* mutant line (*Nkx2-1*^{CreER/CreER}) (left). Note the absence of ventral diencephalic structures (except the supramammillary nucleus), and the relative expansion of the prethalamus in *Nkx2-1* mutants (right).